

## ATBD

### Atmospheric correction

1. Radiative transfer model
2. Rayleigh radiance
3. Calculation of transmittance
  - Aerosol reflectance correction
  - Absorptive aerosol correction
4. Sunlint correction
5. Whitecap correction
6. Turbid water correction
7. Bidirectional Reflectance Distribution Function(BRDF) correction

## 1. Radiative transfer model

The satellite-observed reflectance,  $\rho_T$ , is modeled as follows.

$$L_T(\lambda) = L_M(\lambda) + L_A(\lambda) + L_{MA}(\lambda) + T(\lambda)L_G(\lambda) + t(\lambda)L_{WC}(\lambda) + t(\lambda)L_W(\lambda) \quad (1-1)$$

where  $\lambda$  is wavelength,  $L_M$  is radiance due to gas molecules,  $L_A$  is aerosol radiance,  $L_{MA}$  is radiance due to the interaction between molecules and aerosol particles,  $L_G$  is the radiance resulting from the specular reflection by the direct sun light,  $L_{WC}$  is the radiance resulting from the whitecap,  $L_W$  is water-leaving radiance,  $T$  is the direct transmittance of the atmosphere, and  $t$  is the diffuse transmittance of the atmosphere. Radiance  $L$  and reflectance  $\rho$  is easily converted with each other by the following relation,

$$\rho(\lambda) = \frac{\pi L(\lambda)}{F_0(\lambda) \cdot \cos \theta_0}$$

where  $F_0$  is extraterrestrial solar irradiance, and  $\theta_0$  is the solar zenith angle for that pixel.

The spectral variation in  $L_t$  in the near infrared is used to provide information concerning the aerosol's optical properties. The Rayleigh-scattering component is then removed, and the spectral variation of the remainder is compared with that produced by a set of candidate aerosol models in order to determine which two models of the candidate set are most appropriate. We implemented tables that store the relationship between aerosol reflectance  $\rho_A + \rho_{MA}$  and aerosol single scattering reflectance  $\rho_{AS}$  for each band. The magnitude of  $\rho_A + \rho_{MA}$  in the shorter wavelength bands is estimated from the spectral ratio of aerosol reflectance between two NIR bands. Since the spectral dependency of  $\rho_A + \rho_{MA}$  is dependent on aerosol type.

First, initial values for chlorophyll-a concentration (CHL), total suspended matter (TSM), and absorption of colored dissolved organic matter (CDOM) were defined. Water-leaving reflectance at the NIR bands is then estimated from these values before atmospheric correction was performed. In high turbid area, Water-leaving reflectance at the NIR bands is estimated from high turbid water correction shown Section 7. After the first atmospheric correction, the new water-leaving reflectance was estimated from the obtained CHL, TSM, and CDOM, with atmospheric correction repeated until these values converged. We set the threshold for the convergence condition as the stage at which the difference in CHL between, before and after processing was less than 1%, the difference in SS was less than 0.01 g/m<sup>3</sup>, and the difference in CDOM was less than 0.001 m<sup>-1</sup>. A total of ten iterations were performed.

## 2. Calculation of the air molecule scattering radiance due to molecules (L<sub>M</sub>)

The radiance due to the scattering by atmospheric molecule, L<sub>M</sub>(λ), is calculated by using lookup tables. The lookup tables give ρ<sub>M</sub>(λ) for the given θ(λ), θ<sub>0</sub> and Δφ. To reduce storage, the azimuthal dependence of the reflectance was determined through Fourier analysis and the lookup tables store only the Fourier coefficients. The lookup tables of Fourier Coefficients(ρ<sub>i</sub>(λ,θ(λ),θ<sub>0</sub>)) has 41 values for satellite zenith angle (0.0° - 89.95°) and 45 values for solar zenith angle in 2° increments (0.0° - 88.0°). If there is no exact Fourier Coefficients for the target pixel in the lookup table the values needed are interpolated by two-dimensional linear interpolation.

The lookup tables were constructed by solving the Radiative Transfer Model at standard atmospheric pressure and the absorption of ozone layer was not taken into account. At this stage, we correct the pressure impact with aid of the pressure ancillary data.

ρ<sub>M</sub>(λ) in consideration of pressure impact is calculated by the following equation:

$$\rho_M(\lambda) = \frac{1 - \exp(-\tau_M(\lambda)/\cos\theta(\lambda))}{1 - \exp(-\tau_{M0}(\lambda)/\cos\theta(\lambda))} * \sum_{i=0}^2 \rho_i(\lambda, \theta(\lambda), \theta_0) \cos(i * \Delta\phi(\lambda)) \quad (2-1)$$

τ<sub>M</sub>: Rayleigh optical thickness

τ<sub>M0</sub>: Rayleigh optical thickness at standard atmospheric pressure.  
τ<sub>M0</sub> at each band is shown below.

θ: zenith angle of the satellite

θ<sub>0</sub>: zenith angle of the sun

ρ<sub>i</sub>: Fourier Coefficients which are calculated from lookup tables

Δφ: difference between the solar and the satellite azimuth angles

The Rayleigh optical thickness, τ<sub>M</sub>, is calculated by the following equations:

$$\tau_M(\lambda) = \frac{P}{P_0} \tau_{M0}(\lambda) \quad (2-2)$$

P: atmospheric pressure at each pixel.

P<sub>0</sub>: standard atmospheric pressure (= 1013.25hPa)

τ<sub>M0</sub>(λ): Rayleigh optical thickness at standard atmospheric pressure.  
τ<sub>M0</sub> at each band is shown below.

Band	Rayleigh optical thickness	Band	Rayleigh optical thickness
VN1	0.4467	VN9	0.02571
VN2	0.3189	VN10	0.01525
VN3	0.2361	VN11	0.01525
VN4	0.1559	SW1	0.007107

VN5	0.1132	SW2	0.002380
VN6	0.08714	SW3	0.001246
VN7	0.04265	SW4	0.001246
VN8	0.04265		

## 2.1 Lookup tables for the reflectance due to Rayleigh scattering

The lookup table of each band gives  $\rho_M(\lambda)$  for 3 parameters, i.e.,  $\theta(\lambda)$ ,  $\theta_0$  and  $\Delta\phi$ . In order to reduce volume of the LUT, the azimuthal dependence of the reflectance was determined through two-dimensional Fourier analysis and the Fourier coefficients were stored in the LUT.

$\rho_M(\lambda)$  is calculated by the following equation:

$$\rho_M = \sum_{i=0}^2 \rho_i(\lambda, \theta(\lambda), \theta_0) \cos(i * \Delta\phi(\lambda))$$

$\theta$ : a zenith angle of the satellite

$\theta_0$ : a zenith angle of the sun

$\rho_i$ : Fourier coefficients which are calculated from lookup tables

$\Delta\phi$ : a difference between the solar and the satellite azimuth angles

### (1) Calculation

The tables were calculated for the following values of the independent variables and conditions:

- $\theta$  : 0.0° - 89.95°(41 points)
- $\theta_0$  : 0.0° - 88.0° in 2° increments
- The optical thickness of Rayleigh scattering at standard atmospheric pressure ( $\tau_{r0}$ ) for each band was computed by the following equation (Bodhaine, 1999).

$$\tau_{r0}(\lambda) = 0.0021520 \left( \frac{1.0455996 - 341.29061\lambda^{-2} - 0.90230850\lambda^2}{1 + 0.0027059889\lambda^{-2} - 85.968563\lambda^2} \right) \quad (2-3)$$

$\lambda$  : wavelength( $\mu\text{m}$ )

- Atmospheric pressure : standard atmospheric pressure(1013.25hPa)
- The polarization was considered.
- The absorption of ozone layer was ignored.
- The multiple scattering due to the interaction between molecules and aerosol particles was considered.
- The sea surface was assumed to be flat.

- A plane parallel atmosphere divided into several homogeneous sublayers was assumed.
- Reflectance due to sun glint was removed.
- Response function was considered.

### 3. Calculation of transmittance

#### 3.1 Molecular transmittance

The molecular transmittance is obtained by following equation.

$$t_M(\lambda) = \exp\left(-\frac{\tau_M(\lambda)}{2 \cos x}\right) \quad (3-1)$$

x :  $\theta(\lambda)$  or  $\theta_0$

$\tau_M(\lambda)$  : molecular optical thickness

#### 3.2 Ozone absorption correction

The ozone transmittance is obtained by following equation.

$$t_{oz}(\lambda) = \exp\left\{\frac{-\tau_{oz}(\lambda)}{\cos x}\right\} \quad (3-2)$$

x :  $\theta(\lambda)$  or  $\theta_0$

$\tau_{oz}(\lambda)$  : optical thickness of ozone

$$\tau_{oz}(\lambda) = DU \cdot K_{oz}(\lambda) \quad (3-3)$$

$K_{oz}(\lambda)$  : coefficients which relate optical thickness of ozone and DU.

$K_{oz}$  is calculated beforehand (Table 3-1)

DU : Total ozone. DU(Dobson Unit) means total ozone concentration at 0°C, 1hPa (above mean sea level) and one DU is equal to a hundredth of the ozone layer thickness. DU at each band is shown below.

Table 3-1 Coefficients which relate optical thickness of ozone and DU

Band	$\langle K_{oz}(\lambda) \rangle [DU^{-1}]$	Band	$\langle K_{oz}(\lambda) \rangle [DU^{-1}]$
VN1	TBD	VN9	TBD
VN2	TBD	VN10	TBD
VN3	TBD	VN11	TBD
VN4	TBD	SW1	TBD
VN5	TBD	SW2	TBD
VN6	TBD	SW3	TBD
VN7	TBD	SW4	TBD
VN8	TBD		

#### 3.3 NO<sub>2</sub> absorption correction

The nitrogen dioxide transmittance is obtained by following equation.

$$t_{NO_2}(\lambda) = e^{-k_{NO_2}(\lambda) \cdot NO_2} \quad (3-4)$$

Table 3-2 Coefficients which relate optical thickness of NO<sub>2</sub>

Band	<K <sub>NO<sub>2</sub></sub> (λ)>	Band	<K <sub>NO<sub>2</sub></sub> (λ)>
VN1	TBD	VN9	TBD
VN2	TBD	VN10	TBD
VN3	TBD	VN11	TBD
VN4	TBD	SW1	TBD
VN5	TBD	SW2	TBD
VN6	TBD	SW3	TBD
VN7	TBD	SW4	TBD
VN8	TBD		

### 3.4 Oxygen absorption correction

The O<sub>2</sub> A-band absorption usually reduces more than 10–15% of the measured radiance at the SGLI 763nm band. Ding and Gordon (1995) proposed a numerical scheme to remove the O<sub>2</sub> A-band absorption effects on the SeaWiFS atmospheric correction.

$$t_{O_2}(763) = \frac{1}{1 + 10^{a+b \cdot M + cM^2}} \quad (3-5)$$

where

M : airmass

a = 21.3491, b = 10.1155, and c = 27.0218 3x 10<sup>-3</sup>.

## 4. Calculation of the aerosol scattering radiance due to molecules ( $L_A$ )

### 4.1 Overview

The spectral variation in  $L_t$  in the near infrared is used to provide information concerning the aerosol's optical properties. The Rayleigh-scattering component is then removed, and the spectral variation of the remainder is compared with that produced by a set of candidate aerosol models in order to determine which two models of the candidate set are most appropriate. First, initial values for chlorophyll-a concentration (CHL), total suspended matter (TSM), and absorption of colored dissolved organic matter (CDOM) were defined. Water-leaving reflectance at the NIR bands is then estimated from these values before atmospheric correction was performed. In high turbid area, Water-leaving reflectance at the NIR bands is estimated from high turbid water correction shown Section 7.

We implemented tables that store the relationship between aerosol reflectance  $\rho_A + \rho_{MA}$  and aerosol single scattering reflectance  $\rho_{AS}$  for each band. The magnitude of  $\rho_A + \rho_{MA}$  in the shorter wavelength bands is estimated from the spectral ratio of aerosol reflectance between two NIR bands. Since the spectral dependency of  $\rho_A + \rho_{MA}$  is dependent on aerosol type.

After the first atmospheric correction, the new water-leaving reflectance is estimated from the obtained CHL, TSM, and CDOM, with atmospheric correction repeated until these values converged. We set the threshold for the convergence condition as the stage at which the difference in CHL between, before and after processing was less than 1%, the difference in TSM was less than 0.01 g/m<sup>3</sup>, and the difference in CDOM was less than 0.001 m<sup>-1</sup>. A total of ten iterations were performed.

The aerosol reflectance is corrected through these processes.

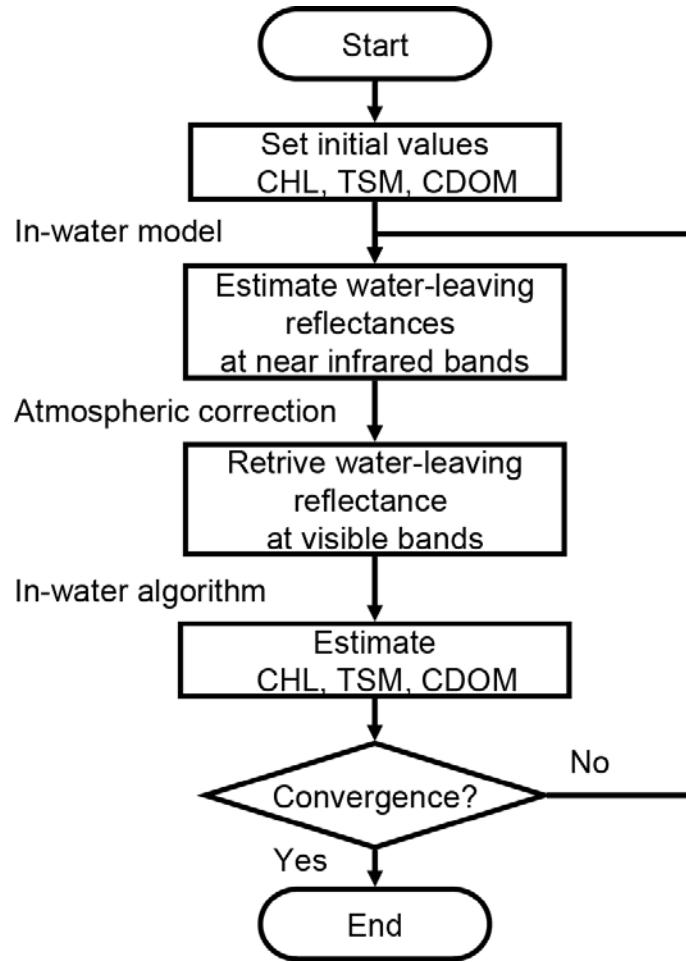


Figure 4.1 Flowchart of iteration procedure

#### 4.2 Determination of aerosol type from near infrared bands

$\rho_A(670) + \rho_{MA}(670)$  and  $\rho_A(865) + \rho_{MA}(865)$  at near infrared bands are calculated by the following equation where  $\rho_W(\lambda)$  is calculated by using in-water model.

$$\rho_A(\lambda) + \rho_{MA}(\lambda) = \rho_T(\lambda) - \rho_M(\lambda) - t(\lambda) \rho_G(\lambda) - t(\lambda) \rho_W(\lambda) \quad (4-1)$$

Then  $\tau_A(M, 670)$  and  $\tau_A(M, 865)$  are obtained by following equation.

$$X = \rho_A(M, \lambda, \theta, \theta_0, \Delta\phi) + \rho_{MA}(M, \lambda, \theta, \theta_0, \Delta\phi)$$

$$\tau_A(M, \lambda, \theta, \theta_0, \Delta\phi) = a_0 + a_1X + a_2X^2 + a_3X^3 + a_4X^4 \quad (4-2)$$

M: aerosol model

$\lambda$ : wavelength

$\theta$ : a zenith angle of the satellite

$\theta_0$ : a zenith angle of the sun

$\Delta\phi$ : a difference between the solar and the satellite azimuth angles

$a_0, a_1, a_2, a_3$  and  $a_4$ : These values are provided by the lookup tables.

### 4.3 Lookup tables for the reflectance due to aerosol scattering

The lookup table of each NIR band and aerosol model contains coefficients  $a_0$ ,  $a_1$ ,  $a_2$ ,  $a_3$  and  $a_4$  of the following equation.

$$X = \rho_A(M, \lambda, \theta, \theta_0, \Delta\phi) + \rho_{MA}(M, \lambda, \theta, \theta_0, \Delta\phi)$$
$$\tau_A(M, \lambda, \theta, \theta_0, \Delta\phi) = a_0 + a_1X + a_2X^2 + a_3X^3 + a_4X^4 \quad (4-2)$$

- M: aerosol model
- $\theta$ : a zenith angle of the satellite
- $\theta_0$ : a zenith angle of the sun
- $\Delta\phi$ : a difference between the solar and the satellite azimuth

angles

On the other hand, the lookup table of each visible band and aerosol model contains coefficients  $b_0$ ,  $b_1$ ,  $b_2$ ,  $b_3$  and  $a_4$  of the following equation.

$$X = \tau_A(M, \lambda, \theta, \theta_0, \Delta\phi)$$
$$\rho_A(M, \lambda, \theta, \theta_0, \Delta\phi) + \rho_{MA}(M, \lambda, \theta, \theta_0, \Delta\phi) = b_0 + b_1X + b_2X^2 + b_3X^3 + b_4X^4 \quad (4-3)$$

- M: aerosol model
- $\theta$ : a zenith angle of the satellite
- $\theta_0$ : a zenith angle of the sun
- $\Delta\phi$ : a difference between the solar and the satellite azimuth

angles

#### (1) Calculation

The tables were calculated for the following values of the independent variables and conditions:

- $\theta$  and  $\theta_0$  :  $0.0^\circ - 80.5^\circ$  in  $3.5^\circ$  increments
- $\Delta\Phi$  :  $0.0^\circ - 180.0^\circ$  in  $4^\circ$  increments
- aerosol models :
  - (Under study)
- $\tau_A$  :
  - (Example)
  - Ocnic50 RH83%
  - 0.001,0.002,0.003,0.004,0.005,0.006,0.007,0.008,0.028,0.050,0.075,0.104,
  - 0.138,0.180,0.234,0.309,0.437
- Atmospheric pressure : standard atmospheric pressure(1013.25hPa)
- The polarization was ignored.
- The absorption of ozone layer was ignored.

- The multiple scattering due to the interaction between molecules and aerosol particles was considered.
- The sea surface was assumed to be flat.
- A plane parallel atmosphere divided into several homogeneous sublayers was assumed.
- Reflectance due to sun glint was removed.
- Response function was considered.

## (2) Interpolation

It uses Lagrange's interpolation for sun and satellite zenith angles and azimuth angle difference which are not covered in the tables. When  $60^\circ \geq \theta$  and  $60^\circ \geq \theta_0$  one degree Lagrange's interpolation is used to obtain  $a_n$ . And when  $\theta > 60^\circ$  or  $\theta_0 > 60^\circ$  two degree Lagrange's interpolation is used.

(2-1) Calculation formula for one degree Lagrange's interpolation (when  $60^\circ \geq \theta$  and  $60^\circ \geq \theta_0$ )

$$a_n(\theta, \theta_0, \Delta\phi) = \sum_{i=u}^{u+1} \sum_{j=v}^{v+1} \sum_{k=w}^{w+1} A_{n,ijk} \cdot L_i(\theta) \cdot M_j(\theta_0) \cdot N_k(\Delta\phi) \quad (4-4)$$

The condition of the grid point numbers,  $u$ ,  $v$  and  $w$ , are as follows.

$$u < \theta < u + 1$$

$$v < \theta_0 < v + 1$$

$$w < \Delta\phi < w + 1$$

where

$$0 \leq u \leq 22, 0 \leq v \leq 22, 0 \leq w \leq 44$$

$A_{n,ijk}$ : values in grid points  $i, j, k$ . It's obtained from the lookup table.

$\theta$ : the zenith angle of the satellite. 0 - 80.5°, 3.5° increments, 24 data,  
 $i = 0, \dots, 23$

$\theta_0$ : the zenith angle of the sun. 0 - 80.5°, 3.5° increments, 24 data,  
 $j = 0, \dots, 23$

$\Delta\phi$ : the difference between the solar and the satellite azimuth angles.  
 0 - 180.0°, 4.0° increments, 46 data,  $k = 0, \dots, 45$

$$L_u(\theta) = \frac{(\theta - \theta_{u+1})}{(\theta_u - \theta_{u+1})} \quad (4-5)$$

$$L_{u+1}(\theta) = \frac{(\theta - \theta_u)}{(\theta_{u+1} - \theta_u)}$$

The shape of equations  $M_j(\theta_0)$  and  $N_k(\Delta\phi)$  are the same as those of  $L_i(\theta)$ .

(2-2) Calculation formula for two degree Lagrange's interpolation (when  $\theta > 60^\circ$  or  $\theta_0 > 60^\circ$ )

$$a_n(\theta, \theta_0, \Delta\phi) = \sum_{i=u}^{u+2} \sum_{j=v}^{v+2} \sum_{k=w}^{w+2} A_{n,ijk} \cdot L_i(\theta) \cdot M_j(\theta_0) \cdot N_k(\Delta\phi) \quad (4-6)$$

$u+1, v+1, w+1$  : grid points closest to  $\theta, \theta_0, \Delta\phi$

where

$$0 \leq u \leq 21, 0 \leq v \leq 21, 0 \leq w \leq 43$$

$A_{n,ijk}$ : values at grid point  $i, j, k$ . It's obtained from the lookup table.

$\theta$ : the zenith angle of the satellite.  $0 - 80.5^\circ, 3.5^\circ$  increments, 24 data,  $i = 0, \dots, 23$

$\theta_0$ : the zenith angle of the sun.  $0 - 80.5^\circ, 3.5^\circ$  increments, 24 data,  $j = 0, \dots, 23$

$\Delta\phi$ : the difference between the solar and the satellite azimuth angles.  $0 - 180.0^\circ, 4.0^\circ$  increments, 46 data,  $k = 0, \dots, 45$

$$L_u(\theta) = \frac{(\theta - \theta_{u+1})(\theta - \theta_{u+2})}{(\theta_u - \theta_{u+1})(\theta_u - \theta_{u+2})}$$

$$L_{u+1}(\theta) = \frac{(\theta - \theta_u)(\theta - \theta_{u+2})}{(\theta_{u+1} - \theta_u)(\theta_{u+1} - \theta_{u+2})}$$

$$L_{u+2}(\theta) = \frac{(\theta - \theta_u)(\theta - \theta_{u+1})}{(\theta_{u+2} - \theta_u)(\theta_{u+2} - \theta_{u+1})} \quad (4-7)$$

The shape of equations  $M_j(\theta_0)$  and  $N_k(\Delta\phi)$  are the same as those of  $L_i(\theta)$ .

#### 4.4 Outline of the algorithm

The pixel-wise procedure for the atmospheric correction is described as follows. In what follows,  $\varepsilon'(M)$  means the estimated value of the spectral ratio of  $\omega_{ATPA}$  between 670 and 865nm bands for an assumed aerosol model  $M$ , while  $\varepsilon(M)$  is the theoretically

derived value of  $\omega_A K_{EXT} P_A$  ratio for a model M.

- (1) Get  $\rho_A(\lambda) + \rho_{MA}(\lambda) = \rho_T(\lambda) \cdot \rho_M(\lambda)$  at 670 and 865nm.
- (2) Estimate  $\tau_A$  at 670nm and 865nm bands for each assumed aerosol model(M) by solving the biquadratic equation in reference to the aerosol LUTs (LookUp Table).
- (3) Calculate  $\varepsilon'_{ave}$  and select a pair of aerosol models A and B, such that  $\varepsilon(A) < \varepsilon'_{ave}$  and  $\varepsilon(B) > \varepsilon'_{ave}$ , by the iteration scheme. Define interpolation ratio r as  $(\varepsilon'_{ave} - \varepsilon(A)) / (\varepsilon(B) - \varepsilon(A))$ .
- (4) For models A and B, obtain  $\tau_A(\lambda, M)$  for band VN1 to 7 by

$$\tau_A(\lambda, M) = \frac{K_{ext}(\lambda, M)}{K_{ext}(865, M)} \tau_A(865, M) \quad (4-8)$$

Derive  $\rho_A(\lambda) + \rho_{MA}(\lambda)$  for the models A and B in use of the aerosol LUT.

- (5) Obtain final  $\rho_A(\lambda) + \rho_{MA}(\lambda)$  by interpolating the  $\rho_A + \rho_{MA}$  values for the models A and B.

#### 4.5 Detection method of absorptive aerosol

In this section, we show detection method of absorptive aerosol. The band of wavelength that is shorter than 550 nm is needed to detect absorptive aerosol. We use 380nm band (SGLI band VN1) to detect it. The water-leaving reflectance at 380 nm ( $\rho_w(380)$ ) isn't contributed by TSM (Han, 1997), though the variance by CHL and CDOM is large.

We define magnitude of aerosol absorption (aalb) as

$$aalb(\lambda) = \frac{[\rho_A(\lambda) + \rho_{MA}(\lambda)]}{\rho_A(\lambda) + \rho_{MA}(\lambda)} \quad (4-9)$$

where  $\rho_A(\lambda) + \rho_{MA}(\lambda)$  is calculated from selected model based on the NIR bands.  $[\rho_A(\lambda) + \rho_{MA}(\lambda)]$  is calculated from eq.(4-1) at SGLI VN1(380nm) by estimating water reflectance. When the absorption is significantly large, the  $[\rho_A(380) + \rho_{MA}(380)]$  becomes much different from  $\rho_A(380) + \rho_{MA}(380)$ . In other words, the absorptive aerosol is detected from the difference, and is corrected by a spectral absorption model.

##### 4.5.1 Spectral dependency of aerosol absorption estimated from satellite data

Effect of aerosol absorption to the satellite data is investigated in this section. Heavy smoke from Siberia forest covered around Japan May 19 to May 26 in 2003<sup>1</sup>. GLI scenes of the smoke were fourteen during this period. Spectral dependency of aalb was estimated by using these scenes. The  $[\rho_A(\lambda) + \rho_{MA}(\lambda)]$  was calculated to assuming CHL of 1mg/m<sup>3</sup>, no sunglint and whitecap. Figure 4.2 shows the average wavelength dependency of aalb. The absorption of smoke aerosol is much larger in shorter

wavelength.  $[\rho_A(\lambda)+\rho_{MA}(\lambda)]$  in 380nm was smaller about 28% than  $\rho_A(\lambda)+\rho_{MA}(\lambda)$  from selected model based on the NIR bands.

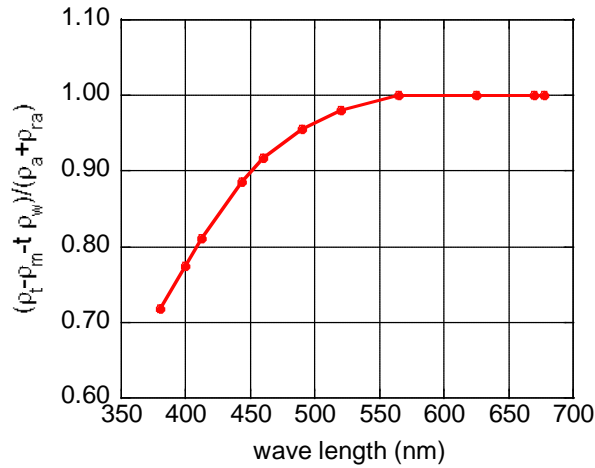


Figure 4.2 Spectral dependency of magnitude of aerosol absorption

### 3.3 Implement of absorptive aerosol correction to atmospheric correction scheme

aalb at 380nm is calculated from  $[\rho_A(380)+\rho_{MA}(380)]$  and  $\rho_A(380)+\rho_{MA}(380)$ .  $[\rho_A(380)+\rho_{MA}(380)]$  is calculated from eq.(4-1) by using water reflectance which was estimated by in-water model of Tanaka et al. (2004). If aalb(380) is less than 1, absorptive aerosol correction is done.

aalb( $\lambda$ ) for other bands is estimated by the following expression.

$$aalb(\lambda) = \{1 - w(\lambda)\} + w(\lambda) \cdot aalb(380), \quad (5)$$

where  $w(\lambda)$  is weight of absorption. It is determined based on empirically from figure 4.2. We assume that  $w(\lambda)$  remains the same for all scenes although aalb( $\lambda$ ) will change from pixel to pixel. Table 1 shows  $w(\lambda)$  values.

Table 4.1 Weight of absorption in atmospheric correction

wavelength(nm)	380nm	412nm	443nm	490nm	530nm	>670nm
$w(\lambda)$	1.0000	0.6694	0.4016	0.1594	0.0360	0.0000

## 5. Sunlint correction

Reflectance of sun glint is calculated by following equations. If  $\rho_G(865)\cos\theta_0 \geq TBD$ , that pixel is masked as sun glint.

$$\rho_G(\lambda) = \frac{\pi f(\omega, \lambda) \cdot t_0(\lambda) \cdot P_W(\theta, \theta_0, \phi, \phi_0, W)}{4 \cdot \cos\theta \cdot \cos\theta_0 \cos^4\theta_n}$$

where

$t_0(\lambda)$  : total downward diffuse transmittance. For near infrared band (749nm and 865nm), it is assume that  $t_0(\lambda)$  is only contributed by molecule. The contribution of aerosol is ignored because aerosol type is unknown.

$$t_0(\lambda) = t_{0,M}(\lambda) \cdot t_{0,A}(\lambda)$$

$t_{0,M}$  : downward diffuse transmittance of molecule

$t_{0,A}$  : downward diffuse transmittance of aerosol

$P_W(\theta, \theta_0, \Delta\phi, W)$  : probability of seeing sun

$$P_W(\theta, \theta_0, \phi, \phi_0, W) = \frac{1}{\pi\sigma^2} \exp\left(\frac{-\tan^2\theta_n}{\sigma^2}\right)$$

$$\sigma^2 = 0.003 + 0.00512W.$$

$$\theta_n = \cos^{-1}\left(\frac{\cos\theta + \cos\theta_0}{2\cos\omega}\right)$$

$$\cos 2\omega = \cos\theta \cos\theta_0 + \sin\theta \sin\theta_0 \cos(\phi - \phi_0).$$

$\theta, \phi$  : satellite zenith and azimuth angle at typical band

$\theta_0, \phi_0$  : solar zenith and azimuth angle at typical band

$W$  : wind speed (m/s)

$\lambda$  : wavelength

$f(\lambda)$  : Fresnel reflectance

$$f(\omega, \lambda) = 1 - (2 \cdot n \cdot y \cdot z) \cdot \cos\omega$$

$n(\lambda)$  : refractive index

$\omega$  : incident angle

$$y = \sqrt{n(\lambda)^2 + \cos^2\omega} - 1/n$$

$$z = \frac{1}{\{\cos\omega + y \cdot n(\lambda)\}^2} + \frac{1}{\{y + n(\lambda)\cos\omega\}^2}.$$

When  $\rho_G(\lambda)\cos\theta_0 \geq TBD$  aaa, the pixel is masked.

## 6. Whitecap correction

The estimation of whitecap reflectance follows the form

$$t(\lambda)L_{WC}(\lambda) = t(\lambda) \cdot t_0(\lambda) \cdot c(\lambda) \cdot R_{WC} \cdot W$$

where  $c(\lambda)$  is wavelength dependent factor (Frouin et al., 1996).

The Koepke effective reflectance for whitecaps ( $R_{WC}$ ) is 0.22.  $W$  is whitecap coverage.

$W$  depend on wind speed. It was explained by Stramska and Petelski(2003).

$$W = 8.75 \times 10^{-5} (U_{10} - 6.33)^3,$$

where  $U_{10}$  is 10m wind speed. Minimum wind speed is 6.33 m/s.

Table 6.1 Wavelength dependent factor

Band	$c(\lambda)$	Band	$c(\lambda)$
VN1	1.0	VN9	1.0
VN2	1.0	VN10	0.5
VN3	1.0	VN11	0.5
VN4	1.0	SW1	0.0
VN5	1.0	SW2	0.0
VN6	1.0	SW3	0.0
VN7	1.0	SW4	0.0
VN8	1.0		

## 7. Turbid water correction

Total suspended matter (TSM) is estimated from satellite data at three near infrared (NIR) bands. Satellite radiances at near infrared bands are described following equation assuming single scattering, no sunglint and no whitecap.

$$L_T(667) = L_M(667) + L_A(667) + t(667)L_W(667)$$

$$L_T(748) = L_M(748) + L_A(748) + t(748)L_W(748) \quad (7-1)$$

$$L_T(869) = L_M(869) + L_A(869) + t(869)L_W(869)$$

To decrease unknown parameter, Aerosol radiance  $L_A(\lambda)$  is assumed that

$$L_A(\lambda) \cong \left( \frac{\lambda}{869} \right)^{-\alpha} \frac{F_0(\lambda)}{F_0(869)} L_A(869) \quad (7-2)$$

where

$F_0(\lambda)$  : Extraterrestrial solar irradiance  
 $\alpha$  : Angstrom exponent coefficient

Single scattering albedo and aerosol phase function do not depend on wavelength.

Water-leaving radiance at near infrared bands are relate with total suspended matter concentration. These equation was determined from in-site data in East China Sea.

$$R_{rs}(670) = 0.000561 \cdot TSM^{1.1156}$$

$$R_{rs}(763) = 0.000256 \cdot TSM^{0.823} \quad (7-3)$$

$$R_{rs}(865) = 0.000165 \cdot TSM^{0.794}$$

Remote sensing reflectance ( $R_{rs}$ ) is related to water-leaving radiance ( $L_w$ ).

$$L_W(\lambda) = R_{rs}(\lambda) \cdot F_0(\lambda) \cdot \cos \theta_0 \cdot t_0(\lambda) \quad (7-4)$$

Eqs. (7-2)(7-3)(7-4) is substituted for eqs.(7-1). It becomes the simultaneous equations of three unknown  $L_A(865)$ , TSM and  $\alpha$ .

$$L_T(667) = L_M(667) + \left( \frac{667}{869} \right)^{-\alpha} \frac{F_0(667)}{F_0(869)} \cdot L_A(869) + t(667) \cdot t_0(667) \cdot 0.003345 \cdot TSM^{0.497} \cdot F_0(667) \cdot \cos \theta_0$$

$$L_T(748) = L_M(748) + \left( \frac{748}{869} \right)^{-\alpha} \frac{F_0(748)}{F_0(869)} \cdot L_A(869) + t(748) \cdot t_0(748) \cdot 0.000256 \cdot TSM^{0.823} \cdot F_0(748) \cdot \cos \theta_0$$

$$L_T(869) = L_M(869) + L_A(869) + t(869) \cdot t_0(869) \cdot 0.000165 \cdot TSM^{0.794} \cdot F_0(869) \cdot \cos \theta_0$$

The value of  $L_A(865)$ , TSM and  $\alpha$  is obtained by solving the simultaneous equations.

## **8. Bidirectional reflectance distribution function**

The upwelling radiance below the ocean surface do not form an isotropic radiance field. Morel and Gentili (1993) was shown this nonisotropic character using Monte Carlo simulation.

We calculate bidirectional effect according to the scheme of Morel and Gentile. Please refer to NASA/TM-2003-21621, Rev-Vol III Chapter 4 (Mueller et al., 2003) for details. Look-up tables (DISTRIB\_FQ\_with\_Raman.tar.gz) were obtained over the internet, using anonymous ftp, from [oceane.obs-vlfr.fr](http://oceane.obs-vlfr.fr).

## 9. Ancillary data

Several sets of ancillary data are required for atmospheric correction of SGLI data. We will summarize each ancillary data set required below.

### 9.1 Total ozone

The total ozone concentration (Dobson Units, DU) is required to calculate the ozone optical thickness, and the ozone optical thickness is needed to compute the two way transmittance of  $\tau_M$  and  $\tau_w$  through the ozone layer.

Dobson Units means total ozone concentration at 0 ° C, 1hPa(above mean sea level) and 1 DU is equal to a hundredth of the ozone layer thickness. DU is expressed in mm.

### 9.2 Sea surface pressure

The atmospheric pressure (hPa) is needed to compute the Rayleigh optical thickness that is required for the computation of  $\tau_M$  and the diffuse transmittance of the atmosphere.

### 9.3 Sea surface wind

The sea surface wind speed (m/s) and vector(degree) are required for the construction of a sun glint mask. The sea surface wind speed also will be required for estimation of the whitecap reflectance.

### 9.4 Total NO<sub>2</sub>

The total NO<sub>2</sub> concentration is required to calculate the NO<sub>2</sub> optical thickness, and the NO<sub>2</sub> optical thickness is needed to compute the two way transmittance of  $\tau_M$  and  $\tau_w$ .

## References

Bodhaine, Barry A., Norman B. Wood, Ellsworth G. Dutton, James R. Slusser, 1999: On Rayleigh Optical Depth Calculations. *J. Atmos. Oceanic Technol.*, **16**, 1854–1861.

doi: 10.1175/1520-0426(1999)016<1854:ORODC>2.0.CO;2

Ding K. and H. R. Gordon (1995), Analysis of the influence of O<sub>2</sub> A-band absorption on atmospheric correction of ocean color

imagery, *APPLIED OPTICS*, Vol. 34, No. 12, pp.2068-2080.

Frouin R., M. Schwindling and P.-Y. Deschamps (1996), Spectral reflectance of sea foam in the visible and near-infrared: In situ measurements and remote sensing implications, *J. GEOPHYSICAL RESEARCH*, VOL. 101, NO. C6, PAGES 14,361-14,371.

Gordon and M. Wang (1994), Retrieval of water-leaving radiance and aerosol optical thickness over the oceans with SeaWiFS: a preliminary algorithm , *Applied Optics*, **33**, 443–452.

Han L. (1997): Spectral reflectance with varying suspended sediment concentrations in clear and algae-laden waters, *Photogram. Engineering & Remote Sensing*, **63**, 701-705.

Mueller J. L., A. Morel, R. Frouin, C. Davis, R. Arnone, K. Carder, Z. P. Lee, R. G. Steward, S. Hooker, B. Holben, C. D. Mobley, S. McLean, M. Miller, C. Peitras, G. S. Fargion, K. D. Knobelspiesse, J. Porter and K. Boss (2003), Ocean Optics Protocols For Satellite Ocean Color Sensor Validation, Revision 4, Volume III:Radiometric Measurements and Data Analysis Protocols, CHAPTER 4, NASA/TM-2003-21621, Rev-Vol III, pp.32-59.

Morel, A. and B. Gentili, 1996: Diffuse reflectance of oceanic waters. III. Implication of bidirectionality for the remote sensing problem. *Appl. Opt.*, **35**: 4850-4862.

Stramska, M. and T. Petelski (2003), Observations of oceanic whitecaps in the north polar waters of the Atlantic, *J. Geophys. Res.*, **108C3**, 3086. doi: 10.1029/2002JC001321

Voigt S., J. Orphal, and J. P. Burrows (1999), High-Resolution Reference Data by UV-Visible Fourier-Transform Spectroscopy: 1. Absorption Cross-Sections of NO<sub>2</sub> in the 250-800 nm Range at Atmospheric Temperatures (223-293 K) and Pressures (100-1000

mbar), Chemical Physics Letters, in preparation

Voigt S., J. Orphal, K. Bogumil, and J. P. Burrows (2001), "The Temperature Dependence (203-293 K) of the Absorption Cross-Sections of O<sub>3</sub> in the 230–850 nm region Measured by Fourier-Transform Spectroscopy", *Journal of Photochemistry and Photobiology A: Chemistry*, **143**, 1–9.